

Quantum Chemical Methods to Elucidate the Mechanism of a Diastereoselective Insertion-Addition Reaction of a Chiral Titanium (IV)-Schiff Base-Benzyl Complex with Hydroxyketones

B. G. Ramos ^a and E. V. Castriciones ^{a,b}

^aNatural Sciences Research Institute, University of the Philippines–Diliman
Quezon City, Philippines 1101, bgramos1@up.edu.ph

^bInstitute of Chemistry, University of the Philippines–Diliman
Quezon City, Philippines 1101, evcastriciones@up.edu.ph (corresponding author)

ABSTRACT

We present our preliminary results on the quantum chemical studies carried out to elucidate the diastereoselective insertion-addition reaction of a chiral titanium(IV)-Schiff base-benzyl complex (**I**) with hydroxyketones (**II**) to form the diastereoselective insertion product (**III**) in Figure 1. Calculations were performed within the semiempirical methods GFN2-xTB and PM6 as well as with B3LYP in implicit toluene. Possible reactivity sites were examined by investigating the frontier molecular orbitals and the condensed Fukui functions of the reactants. Based on these reactivity indicators and on a previously proposed mechanism for the reaction, a possible reaction pathway is rationalised. For all levels of theory considered in this work, the transition state leading to the insertion of the hydroxyketone and migration of the benzyl moiety to the ketone, appears to be the rate-determining step for the reaction. The semiempirical methods resulted in a lower activation energy for the transition point compared with B3LYP.

Keywords: insertion/addition reaction, reaction mechanism, organotitanium complex, density functional theory, semiempirical quantum chemistry

1 INTRODUCTION

Schiff bases are a popular class of ligands in coordination chemistry because their complexes continue to find many biomedical and industrial applications particularly in catalytic transformations [1]. These

complexing agents are synthesized from facile condensation of any primary amine with an aldehyde or ketone. Because Schiff bases can be prepared efficiently in high yields, metal complexes of Schiff bases designed as Lewis acid catalysts have been a source of interest among chemist in enantioselective reactions. The catalytic activities of chiral Schiff base complexes are known to be selective in reactions such as oxidation, hydroxylation, aldol condensation, and epoxidation [2–4].

In 2000, Scott and colleagues prepared the first C_2 -symmetric Schiff base ligand from 2,2'-diamino-6,6'-dimethylbiphenyl and 3,5-di-tert-butylsalicylaldehyde [5–7]. The reaction of this ligand with $[Ti(CH_2Ph)_4]$ led to the interesting Ti(IV)salicylbiphenyldiimine-benzyl complex labelled **I** in Figure 1. The bulky and rigid Schiff base ligand creates a highly sterically hindered chiral environment around the Ti^{4+} metal center in complex **I**. The metal center is also coordinately unsaturated with the ligands arranged in a distorted trigonal bipyramidal geometry. The presence of an available coordination site on Ti^{4+} as well as the nucleophilic metal-benzyl bond suggests potential use in stereoselective insertion/addition of hydroxyketones with subsequent stereoselective benzylation of the inserted hydroxyketones.

One of the authors investigated the benzylation/addition reactions of complex **I** with some hydroxyketones in toluene at ambient temperatures for about 12 hours [5]. In particular, the insertion/addition reaction of the complex $[TiL^3(CH_2Ph)]$ with 5-chloro-2-hydroxyacetophenone, as shown in Figure 1, afforded the formation of a six-coordinate insertion product, complex **III**, at an 80% yield with only one diastereomer present (*ca.* 90% *de*).

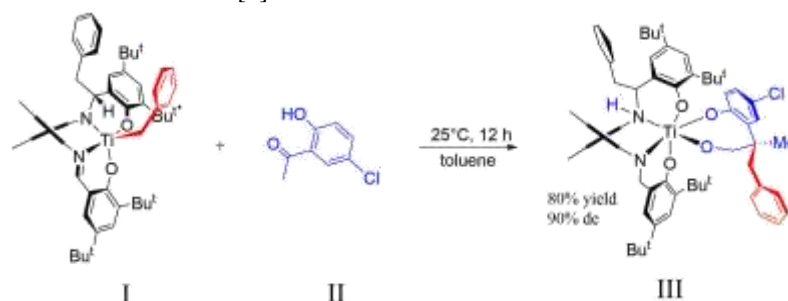


Figure 1. The insertion-addition reaction studied in this work. Complex **I** is titanium(IV)-Schiff base-benzyl complex, molecule **II** is 5-chloro-2-hydroxyacetophenone, and complex **III** is the product of the reaction.

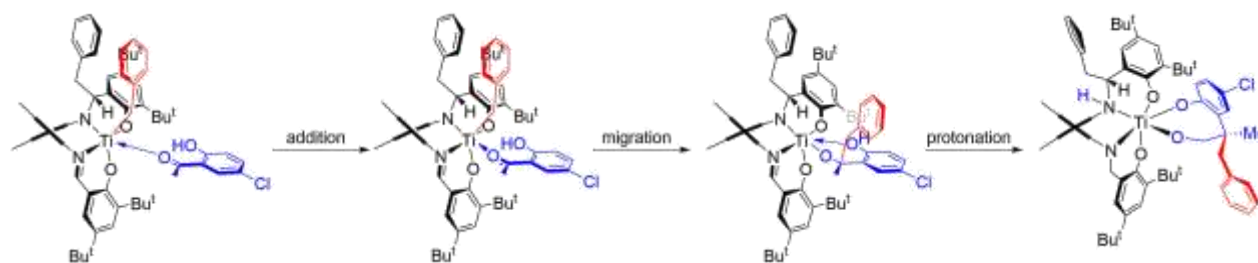


Figure 2. The proposed insertion/addition mechanism for the title reaction.

Castriciones posited an addition/insertion-type of mechanism to explain the observed reaction [5]. The mechanism depicted in Figure 2 consists of three stages: (i) the addition of the incoming hydroxyketone carbonyl oxygen to the metal center via the carbonyl oxygen, (ii) the migration of the benzyl ligand to the partially positive carbonyl carbon of the ketone, and (iii) the coordination of ketone's phenolic oxygen to the Ti^{4+} center with a concurrent donation of the former's proton to the amido nitrogen of the Schiff base. In our best knowledge, the mechanism has not been studied in-depth apart from the initial PM3 computations presented in [5]. In this work, we present our progress toward understanding the title reaction using methods of quantum chemistry. In particular, we report our preliminary from B3LYP/6-31G(d), GFN2-xTB, and PM6 calculations.

2 METHODOLOGY

Guided by the proposed mechanism illustrated in Figure 2, we performed potential energy surface (PES) scans over selected internal coordinates using the software xtb 6.2.3/6.3.2 [8] to identify candidate stationary and transition states. The xtb software implements the GFN2-xTB Hamiltonian, a semiempirical extended tight-binding

method, which has been proven robust in the calculation of thermochemical and transition state properties of complex organic and organometallic reactions [9]. At this computation level, the solvent toluene was accounted for by turning on the option for generalized Born implicit solvation in xtb. In addition to the optimized structures for molecules **I**, **II**, and **III** in Figure 1, five converged structures were found along the path of the proposed mechanism. The geometries are shown Figure 3. These structures are again optimized at the semiempirical PM6 level and at the B3LYP/6-31G(d) level using Gaussian 09 [10] with implicit toluene solvation by means of the polarizable continuum model. Vibrational frequency calculations were performed on all structures at each level of theory to verify that intermediates only possess real frequencies while transition structures exhibit only one imaginary frequency. To assess if the transition states connect with the correct intermediates, intrinsic reaction coordinate (IRC) calculations were performed on structures **2** and **4** of Figure 3. Gaussian 09 was used in all vibrational and IRC analyses. Multiwfn 3.7 [11] was used in the investigation of the Fukui functions and non-covalent interactions.

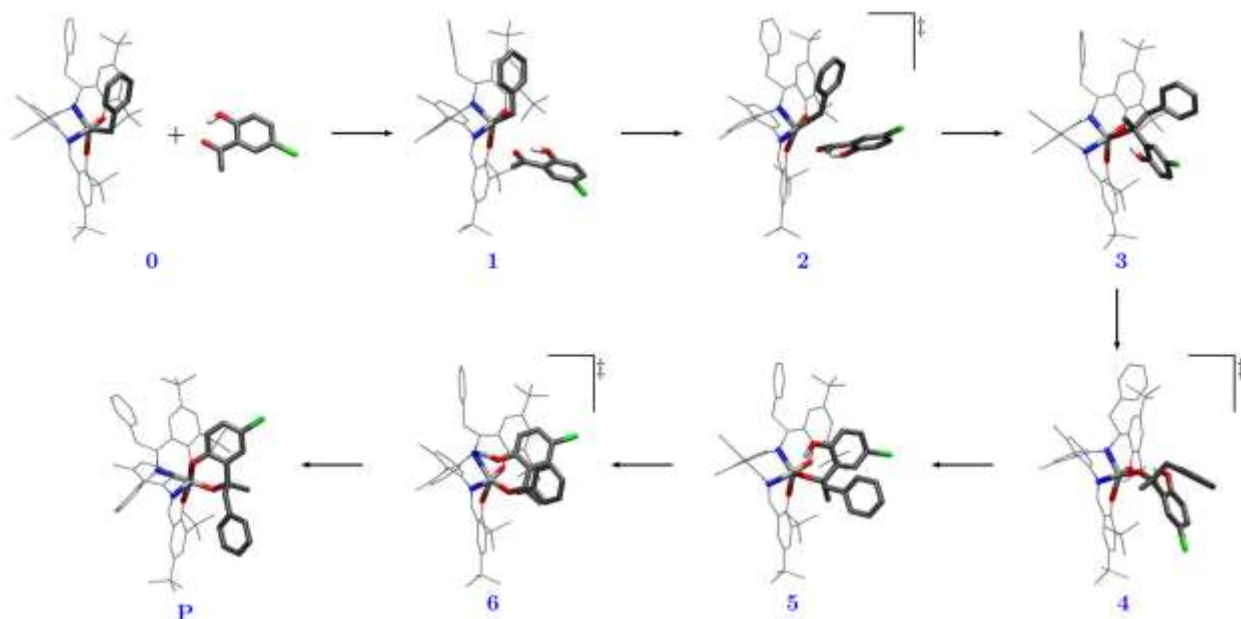


Figure 3. The energy minima and transition points obtained from PES scans of selected internal coordinates at the semiempirical GFN2-xTB level of theory. The Schiff base ligand is represented by gray lines while the benzyl ligand and the hydroxyketone are shown in licorice representation.

3 RESULTS

To determine the probable initial trajectory of the reactants toward successful reactive collisions, reactivity indicators from the frontier molecular orbitals and the Fukui functions were examined. In frontier molecular orbital (FMO) analysis, regions where the highest occupied molecular orbital (HOMO) is confined, are potential electrophilic sites that can attack a nucleophilic region indicated by areas where the lowest occupied molecular orbital (LUMO) is localized. For all QM levels considered in this work, we find that the energy difference of the HOMO of the complex **I** and the LUMO of the ketone **II** is lower than the energy difference of the other MO pair, thus by FMO theory, the reaction must be driven by these molecular orbitals. Figure 4 shows maps of these frontier orbitals calculated at the B3LYP/6-31G(d)-PCM level of theory. Similar MO maps are obtained for PM6-PCM and GFN2-xTB-GBSA (data not shown). Evidently, the phases of complex **I**'s HOMO and the ketone's LUMO have maximum overlap when the ketone attacks below the benzyl ligand. It appears from Figure 4 that the carbonyl oxygen could favorably bind to the metal center while the HOMO electrons of the benzyl attack the carbonyl carbon of the incoming ketone. This deduction from FMO analysis also holds true for the semiempirical levels PM6-PCM and GFN2-xTB-GBSA.

Another powerful local reactivity indicator is the condensed dual descriptor Δf based on the Fukui functions $f^+(\mathbf{r})$ and $f^-(\mathbf{r})$. An atom k acts as an electrophile if $\Delta f_k > 0$ and conversely, acts as a nucleophile if $\Delta f_k < 0$. For the hydroxyketone, the most positive Δf_k value is associated with the carbonyl carbon for all QM levels (data not shown). Apart from the chlorine atom, the most negative Δf_k is obtained for the hydroxyl oxygen in the B3LYP/6-31G(d)-PCM and GFN2-xTB-GBSA computations. In the case of PM6-PCM however, the carbonyl oxygen assumed the most negative Δf_k followed by the methyl substituent, then the hydroxyl oxygen. Nonetheless, the overall picture emerging from this analysis suggests that the carbonyl carbon is prone to electrophilic attack possibly by a nucleophilic group such as the benzyl ligand of complex **II** as implied in the proposed mechanism by Castriciones [5]. To verify that this is the case, analysis of the descriptor Δf for complex **I** shows that the methylenic carbon of the benzyl is nucleophilic for all QM computations. However, only B3LYP/6-31G(d)-PCM correctly ranks the Ti^{3+} metal center as the most electrophilic site by admitting the largest Δf value. PM6-PCM, on the other hand, predicts the metal center to be strongly nucleophilic with a very negative Δf . Nevertheless, remarks regarding the potential of the benzyl ligand to attack the electrophilic carbonyl carbon of the ketone is consistent with our findings from FMO theory.

Given the above diagnostic data about the reactants as well as the mechanism earlier postulated for the reaction, we performed potential energy surface (PES) scans by driving selected internal coordinates along reactive sites

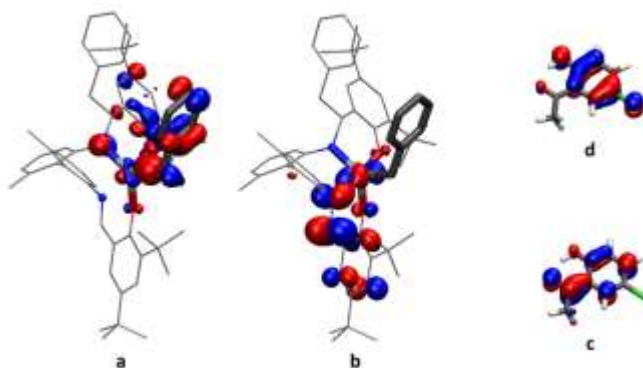


Figure 4. Frontier molecular orbitals of the reactants obtained from B3LYP/6-31G(d)-PCM. (a) HOMO of complex **I**, (b) LUMO of complex **I**, (c) HOMO of ketone **II**, and (d) LUMO of ketone **II**.

toward potential intermediate configurations. Because PES scans are computationally expensive for QM methods beyond the semiempirical level, we decided to carry out the scans at the GFN2-xTB-GBSA and then simply optimized the gathered geometries at the other two QM levels. The relevant configurations along the purported reaction path are shown in Figure 3. Configuration **0** represents the reaction system when the reactants are distant from each other and is designated the reference state (i.e., $\Delta E = 0$ kcal/mol) in the energy profile drawn in Figure 5. The hydroxyketone is then steered to approach the Ti^{4+} center of complex **I** below the benzyl ligand, and state **2** in Figure 5 appeared to be the stable configuration for this event. Following the mechanism in Figure 2, we initially designed a PES scan that would allow the ketone to first bind to the unsaturated metal center and sequentially be followed by a benzylation reaction with the bound ketone. However, even if we change the order of these two stages of the mechanism, we always end up with intermediate **3**. This finding strongly suggests that the addition of the ketone to Ti^{4+} must occur simultaneously with the benzylation of the ketone. Calculation of the intrinsic reaction coordinate from the transition state (TS) **2** at the B3LYP/6-31G(d)-PCM also confirms that this is the case. The TS point **2** is the energy maximum for the entire reaction as shown in Figure 5, and thus the rate-limiting step. GFN2-xTB-GBSA predicts this TS to be surmountable, requiring only a mere 3.3 kcal/mol energy barrier. B3LYP/6-31G(d)-PCM resulted in a calculated activation energy of 33.4 kcal/mol, suggesting that the reaction must occur at a slightly elevated temperature, in contrast to what was observed experimentally in [5]. This discrepancy is rationalised by the inherent limitation of B3LYP theory. While it is deemed sufficient in describing molecular geometries, it may fail in giving accurate energy estimates especially when used with crude basis sets [12]. Efforts are under way to improve on the level of theory being applied in investigating the transition state (as well as alternate reaction channels) such as increasing the basis sets, to provide more details on the observed process of the stereoselective insertion/addition stage of the reaction.

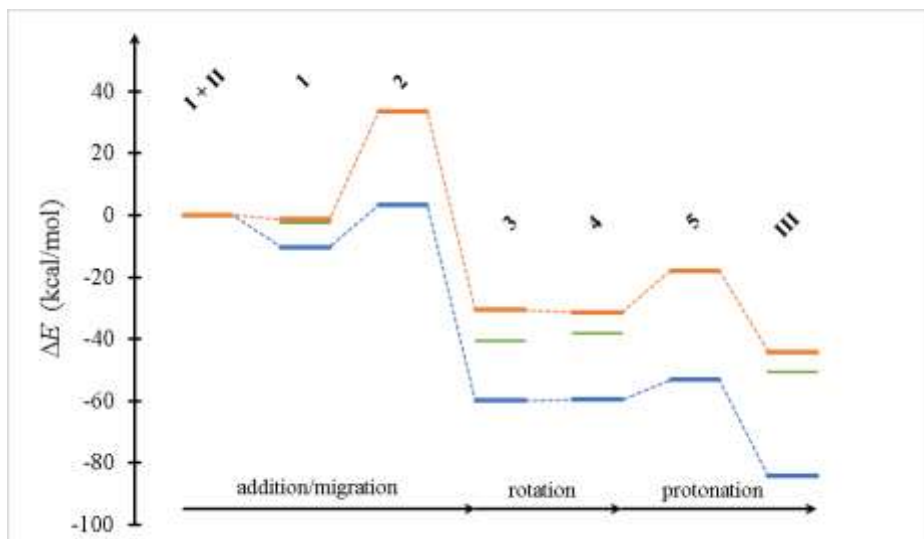


Figure 5. Reaction energy profile for the mechanism computed at the following levels of theory: B3LYP/6-31G(d) (—), GFN2-xTB (—), and PM6 (—) in implicit toluene.

After intermediate **3**, the hydroxyl oxygen of the ketone is posed to attack the metal center to afford state **4**. In completing the process, the hydroxyl moiety donates its hydrogen to the amido nitrogen of the Schiff base ligand to achieve the detected product **III**. For B3LYP/6-31G(d)-PCM and GFN2-xTB-GBSA, this demands an activation complex **5** with a much less energy requirement than TS **2**. We are currently continuing with our computational studies to further refine our data and address the issues we encountered in this preliminary investigation.

The overall reaction energy profile for the investigated mechanism is summarized in Figure 5. Clearly, the semiempirical methods underestimate the relative energies of the relevant points in the reaction path by (at most tenfold for GFN2-xTB-GBSA) compared to B3LYP. Climbing the rate-determining TS **2** is energetically probable at ambient conditions according to GFN2-xTB-GBSA and PM6-PCM but not for B3LYP/6-31G(d)-PCM. Nevertheless, the usefulness of these two semiempirical methods should not be underrated especially for initial treatment of large molecules like the ones regarded here. In fact, for TS **2** alone, the RMSD of the predicted structure by GFN2-xTB-GBSA compared with B3LYP/6-31G(d)-PCM is so small ($\text{RMSD} = 2.6 \times 10^{-4}$) which proves the former can provide nearly high-quality molecular coordinates at considerably lower computational costs.

REFERENCES

- [1] L. Fabbrizzi, "Beauty in Chemistry : Making Artistic Molecules with Schiff Bases," *J. Org. Chem.*, vol. 85, pp. 12212–12226, 2020.
- [2] A. M. Abu-dief and I. M. A. Mohamed, "A review on versatile applications of transition metal complexes incorporating Schiff bases," *Beni-Suef Univ. J. Basic Appl. Sci.*, vol. 4, no. 2, pp. 119–133, 2015.
- [3] J. Zhang, L. Xu, and W. Wong, "Energy materials based on metal Schiff base complexes," *Coord. Chem. Rev.*, vol. 355, pp. 180–198, 2018.
- [4] M. S. More et. al, "Metal complexes driven from Schiff bases and semicarbazones for biomedical and allied applications : a review," *Mater. Today Chem.*, vol. 14, p. 100195, 2019.
- [5] E. Castriciones, "A highly diastereoselective insertion/addition reaction of hydroxyketones into a chiral titanium(IV) Schiff base-benzyl complex," University of the Philippines, Diliman, 2002.
- [6] P. D. Knight et. al, "Problems and solutions for alkene polymerisation catalysts incorporating Schiff-bases; migratory insertion and radical mechanisms of catalyst deactivation †," *Chem. Commun.*, pp. 352–353, 2002.
- [7] P. R. Woodman et. al, "Chiral N₂O₂ Schiff-base complexes of titanium with a biaryl backbone: highly diastereoselective migratory insertion of alkyl at imine," *Dalt. Trans.*, pp. 3340–3346, 2000.
- [8] C. Bannwarth et al. "Extended tight-binding quantum chemistry methods," *WIREs Comput. Mol. Sci.*, no. April, pp. 1–49, 2020.
- [9] S. Dohm et. al, "Semiautomated Transition State Localization for Organometallic Complexes with Semiempirical Quantum Chemical Methods," *J. Chem. Theory Comput.*, vol. 16, no. 3, pp. 2002–2012, 2020.
- [10] M. J. Frisch et. al, "Gaussian 09, Revision A.01." Gaussian, Inc., Wallingford CT, 2009.
- [11] T. Lu and F. Chen, "Multiwfn : A Multifunctional Wavefunction Analyzer," *J. Comput. Chem.*, no. 33, pp. 580–592, 2011.
- [12] R. K. Raju, A. A. Bengalia, and E. N. Brothers, "A unified set of experimental organometallic data used to evaluate modern theoretical methods," *Dalt. Trans.*, no. 45, pp. 13766–13778, 2016.